INTRODUCTION

1. The urgency of the thesis

In order to create a translational motion using traditional electric motor, intermediate mechanisms must be used that leads to the decrease of system performance and accuracy. Moreover, intermediate mechanisms increase the system size and have bad effects on system dynamics due to accumulated error of the system components. Nowadays, translational motion is widely used in industries such as: robots, lifting machines, CNC machine tools... In many applications, the electric drive system must be compact in size due to limited installation space while ensuring flexibility, accuracy and dynamic performances. Linear motor meets all the above requirements because it produces translational motion directly without using intermediate mechanisms like in indirect linear motion systems. Polysolenoid linear motor is a permanent magnet linear synchronous motor with tubular structure. This type of linear motor can fully meet the above requirements that are especially important for parallel robot applications such as hexapod. Therefore, polysolenoid linear motor is chosen to be the subject of the thesis.

2. Subject, scope and method of research

Study subject: The content of the thesis focuses on designing a controller which is able to handle the end effect of permanent magnet polysolenoid linear motor in the control structure. Thesis content includes:

Content 1: Overview study of modeling methods for permanent magnet linear motors in general and then the polysolenoid linear motor in particular. First, a model of the polysolenoid linear motor is built without considering the end effect. Coordinate system transformations are used to gain mathematic model in order to use direct decoupling structure in the control structure.

Content 2: Study on the end effect in linear motors in general (expressed through the structural features of linear motors, physical nature ...). After that, a method for modeling polysolenoid linear motor considering the end effect is proposed. Build the mathematic model of the control object considering the end effect used in the control.

Content 3: Basing on the mathematical model, the control design for the polysolenoid linear motor is conducted. The methods of control design for polysolenoid linear motor is divided into two groups: The first group consists of methods (Min-max CCS, Min-max FCS, Min-max Deadbeat) applied to the model without considering the end effect, the second group (backstepping, adaptive control) is capable of dealing with the end effect of the polysolenoid motor.

Content 4: Proposing the structure and building an experimental system to verify the theoretical research results.

Research scope of the thesis: The thesis focuses on studying characteristics and difficulties when considering the end effect of Polysolenoid motor. Since then, a control structure for polysolenoid linear motion is built. The given characteristics of this complex control object show that there are many challenges in modeling, in analyzing and choosing appropriate control design methods for the object to achieve high accuracy.

Research method: The thesis uses analysis, evaluation and synthesis methods. Through an overview study to find the problem that needs to be solved in theory and design algorithm to solve that problem, verify theoretical studies by simulation and experiment.

3. Objectives of the thesis

The objective of the thesis is to research and control design for electric drive systems using polysolenoid motor considering the end effect. The research objectives in this thesis are as follows:

- Nonlinear dynamic model of polysolenoid motor considering the end effect: the accuracy of the model is a prerequisite for success with any control technique that is based on the model; hence a suitable model of the control object needs to be build in accordance with control design.

- Applying successfully the method of designing the backstepping adaptive controller for the electric drive system using polysolenoid motor. Validate control quality of algorithms by theory and experiment.

4. New contributions, scientific and practical significance of the thesis

The objective of the thesis is to research and control design for electric drive systems using Polysolenoid motor considering the end effect. The research objectives in this thesis are as follows:

New contributions:

- Nonlinear dynamic model of polysolenoid motor considering the end effect: The thesis has built a model of PM polysolenoid linear motor with consideration of the end effect and propose a structural diagram of the motor in which the components affected by the end effect are pointed out.
- Applying successfully the method of designing the backstepping adaptive controller for the electric drive system using polysolenoid motor to handle the end effect. Verify control quality of algorithms by theory and experiment.
- Designing a two closed loop control system in which the inner loop is force control loop (current control loop) that uses the control methods such as Dead-beat, CCS-MPC, FCS-MPC; the outer loop is speed and position control loop which uses Min-max MPC controller.

Scientific and practical significance of the thesis:

The thesis has solved the problem of transferring the theoretical research results into practice through the hardware system built by the author. The thesis has also developed solutions to install flexibly control algorithms to increase the efficiency of hardware usage.

The results of this study can be applied to a class of objects that produce directly linear motion without the use of intermediate mechanical gear boxes especially in parallel robot systems such as hexapod robots

5. The layout of the thesis

The thesis includes the introduction, 04 chapters, conclusions and recommendations, arranged as follows:

Chapter 1. Overview of linear motors and control methods

Chapter 2. Linear motor modeling

Chapter 3. Control the permanent magnet polysolenoid linear motor.

Chapter 4. Simulation and experimental results

Conclusion and Recommendation: The new contributions of the thesis have been highlighted and future works are proposed.

CHAPTER 1 : OVERVIEW OF LINEAR MOTORS AND CONTROL METHODS

1.1 Overview of linear motors

1.1.1 Characteristics of a linear drive system

1.1.2 History of development and application of linear motors

Fig. 1.4 Applications of linear motors.

1.1.3 Structure, working principle and classification of linear motors

With linear motor, the linear motion part can be the stator part or the rotor part of the traditional rotary machine, therefrom corresponding linear motors are created.

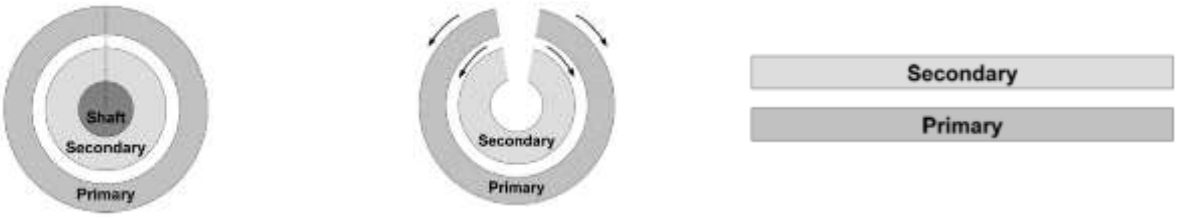

Fig. 1.7 Principle of conversion from a rotary motor to a linear motor.

1.1.4 End effect

The end effect is a characteristic of linear motors which is different in comparison with other types of motors. Since the opened magnetic circuit structure of a linear motor leads to its flux distribution is ununiformed in the air gap, it is unevenly distributed in the middle and two ends. This results in cogging torque, cogging speed in the operation of the motor.

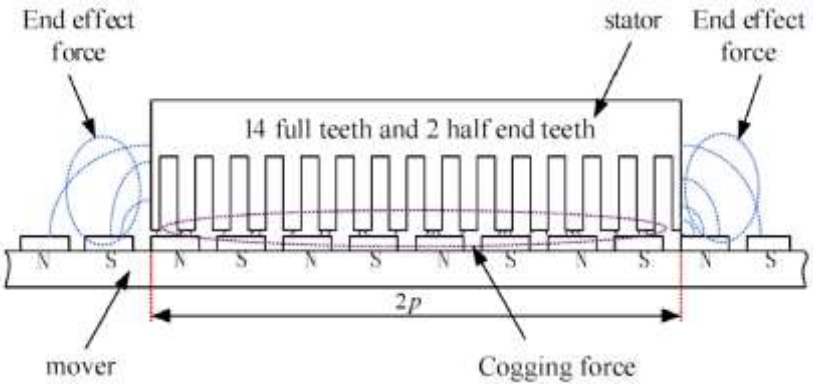

Fig. 1.17 End effect in PLSM flat linear motor [34]

1.2 Linear drive and control methods

1.2.1 Requirements for linear drive control problem

1.2.2 Overview of researches on linear motors

Overview of domestic researches

- About the research works published in domestic scientific journals, there are some articles written on this issue, but only on the level of overview on control methods in theory and simulation in Matlab Simulink.

- The thesis works are experimentally studied on real devices [2.6] published in the form of technical doctoral thesis.

Overview of researches in the world (oversea)

In the last period of time, the group of synchronous linear motors which is mostly focused on is a group of permanent magnet synchronous flat linear motors with short stators corresponding to PM three-phase AC motors.

Issues of interest are studied:

First problem group: Applying the control methods has been successfully applied to rotary motor groups to linear motors.

The second problem group: The method of determining the top of pole of the rotor flux generation axis.

The thirst problem group: Motor modeling.

The forth problem group: Improving control quality.

The fifth problem group: In [31] proposed a method that does not need to identify the end effect using a robust adaptive controller to compensate for uncertainties of end effect, but it still exists the position sensor in the model.

1.3 Polysolenoid linear motor drive system and control methods

1.3.1 Polysolenoid permanent magnet linear motor

Permanent magnet polysolenoid linear motor belongs to the group of permanent magnet synchronous motor with tubular structure; the motor has two phases with two windings arranged in 90 degree difference.

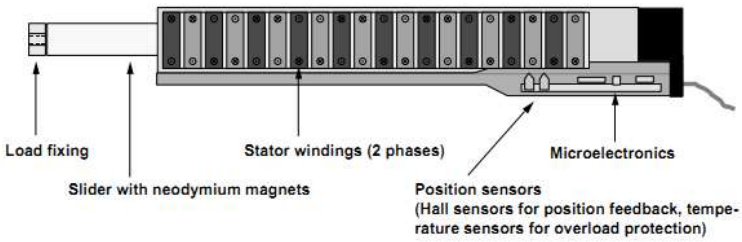

Fig. 1.21 Diagram of internal structure of PM polysolenoid linear synchronous motor [60]

1.3.2 Control of polysolenoid linear motor drive system

Overview of domestic researches:

With reference sources are articles and dissertations stored in the National Library of Vietnam, there is no research work on linear drive control of polysolenoid linear motor.

Overview of researches in the world (oversea)

Studies in the world with short stator linear tubular motors concentrate on a number of problem groups as follows:

• First problem group: Modeling the motor design

• Second problem group: Design of control structures

• Third problem group: Describe the end effect of three-phase tubular linear motors using experimental methods.

In the published works focus on two main directions.

- *The first direction*: Focusing on the end effect with two approaches are equivalent magnetic circuit and using FEM. In the two above methods, the method of using FEM describes end effect more intuitive. However, when using FEM, it is necessary to obtain the exact motor parameters.
- *The second direction*: Study on uncertainty compensating control structure of the end effect. However, the system needs a position sensor.

CONCLUSION OF CHAPTER 1:

The above analysis show that: Linear motor is derived from rotary motor and basically in many cases (design of control structure, analysis of physical phenomena...) the two groups of motors are similar to each other. But in the linear motor, there are characteristics that are not available in the rotary motor such as end effect, which needs further research in the following sections of the thesis. Acquiring knowledge on linear motors helps us accomplish the following objectives:

• Create a basis for the mathematical description process of linear motors.

• Understand the end effect in linear motor, thereby finding ways to handle this phenomenon in the control structure.

The content of section 1.3 focuses on clarifying the study situation of polysolenoid linear motors, problems related to models and control methods of polysolenoid linear motor

drive system. This facilitates the selection and proposal of the next research methods for the control problem of polysolenoid linear drive system.

CHAPTER 2 : LINEAR MOTOR MODELLING

2.1 Mathematic model of the permanent magnet linear synchronous motor

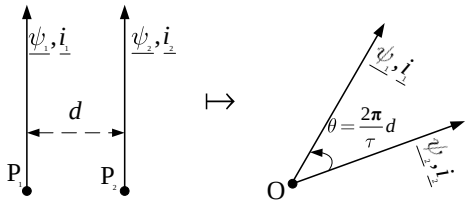

Fig. 2.1 Correlation between vectors in linear motor

State model of LPMSM in *dq* frames (Fig. 2.3) is as follow:

Where, $\mathbf{i}_s^f = \begin{bmatrix} i_{sd} \\ i_{sq} \end{bmatrix}$ and $\mathbf{u}_s^f = \begin{bmatrix} u_{sd} \\ u_{sq} \end{bmatrix}$ satisfy:

$$\frac{d}{dt}\left(\mathbf{i}_s^f\right) = \mathbf{A}^f \mathbf{i}_s^f + \mathbf{B}^f \mathbf{u}_s^f + \mathbf{N}\mathbf{i}_s^f \omega_e + \mathbf{S}\psi_p \omega_e \qquad (2.20)$$

$\mathbf{A}^f$ System matrix.

$$\mathbf{A}^f = \begin{bmatrix} -\frac{1}{T_{sd}} & 0 \\ 0 & -\frac{1}{T_{sq}} \end{bmatrix}$$

$\mathbf{B}^f$ Input matrix.

$$\mathbf{B}^f = \begin{bmatrix} \frac{1}{L_{sd}} & 0 \\ 0 & \frac{1}{L_{sq}} \end{bmatrix}$$

$\mathbf{N}$ Nonlinear coupling matrix.

$$\mathbf{N} = \begin{bmatrix} 0 & \frac{L_{sq}}{L_{sd}} \\ -\frac{L_{sd}}{L_{sq}} & 0 \end{bmatrix}$$

$\mathbf{S}$ Interference matrix.

$$\mathbf{S} = \begin{bmatrix} 0 \\ -\frac{1}{L_{sq}} \end{bmatrix}$$

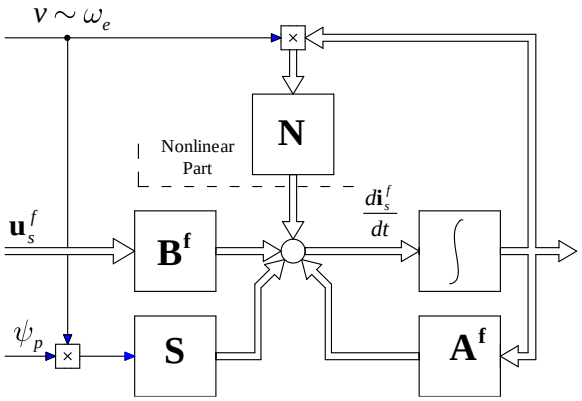

Fig. 2.3 The model of LPMSM in the state space in *dq* coordinate system

2.2 End effect of LPMSM

2.2.1 Introduction to end effect of LPMSM

Linear Permanent Magnet Synchronous Motor (LPMSM) is gradually becoming a popular automation product because it allows the removal of mechanical actuators such as endless screw, belt, etc.. However, the linear motor is affected by the end effect due to opened magnetic circuit structure.

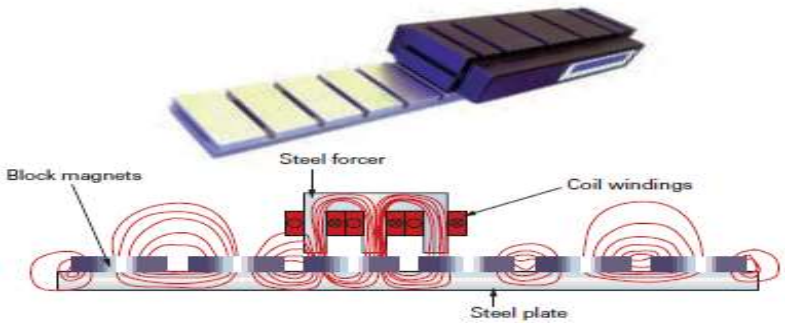

Fig. 2.4 End effect in flat LPMSM

The end effect is understood as the distinction between the beginning and the end areas with the midpoint area of the electromagnetic distribution affecting the flux and force generated by the linear motor (due to the opened magnetic circuit of linear motor). This is reflected in the characteristic: With a permanent stimulating synchronous motor, the magnetic field distribution at the ends of the excitation is reduced illustrated in Fig. 2.4. This varies depending on the speed of motor (magnitude of the excitation current). The suddenly appearance or suddenly end of the inductive side current (corresponding to the appearance or end of the stimulating current). Axial reactions causes a change in the speed of the motor (cogging in speed). This is also a point to be mindful of in linear motors.

2.2.2 End effect in tubular LPMSM

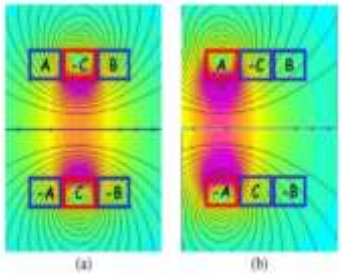

Fig. 2.6 The flux distribution is obtained only when phase C (Fig. a) or only phase A (Fig. b) is energized [18]

$$\begin{bmatrix}\psi_A\\ \psi_B\\ \psi_C\end{bmatrix}=\left(L_0\begin{bmatrix}1&0&0\\0&1&0\\0&0&1\end{bmatrix}+L_2\begin{bmatrix}\cos(2\theta)&0&0\\0&\cos\left(2\theta+\frac{2}{3}\pi\right)&0\\0&0&\cos\left(2\theta-\frac{2}{3}\pi\right)\end{bmatrix}\right)\begin{bmatrix}i_A\\ i_B\\ i_C\end{bmatrix} \tag{2.25}$$

$$+M_2\begin{bmatrix}0&\cos\left(2\theta-\frac{2}{3}\pi\right)&\cos\left(2\theta+\frac{2}{3}\pi\right)\\ \cos\left(2\theta-\frac{2}{3}\pi\right)&0&\cos(2\theta)\\ \cos\left(2\theta+\frac{2}{3}\pi\right)&\cos(2\theta)&0\end{bmatrix}\begin{bmatrix}i_A\\ i_B\\ i_C\end{bmatrix}+M_0\begin{bmatrix}0&1&1\\1&0&1\\1&1&0\end{bmatrix}\begin{bmatrix}i_A\\ i_B\\ i_C\end{bmatrix}+\Delta_{M_0}\begin{bmatrix}0&1&1\\1&0&1\\1&1&0\end{bmatrix}\begin{bmatrix}i_A\\ i_B\\ i_C\end{bmatrix}$$

In the above equation, the component Δ_{M0} represents the end effect in a tubular linear motor. Convert the flux equation to the form in the *dq* frames with transformation (2.18) as follows:

$$\begin{aligned}\psi_d &= \left(L_0+\frac{1}{2}L_2-M_0+M_2+\frac{2}{3}\Delta_{M_0}\left(1-\cos\left(2\theta-\frac{2}{3}\pi\right)\right)\right)i_d-\frac{2}{3}\Delta_{M_0}\sin\left(2\theta-\frac{2}{3}\pi\right)i_q \\ \psi_q &= \left(L_0-\frac{1}{2}L_2-M_0+\frac{2}{3}\Delta_{M_0}\left(1-\cos\left(2\theta-\frac{2}{3}\pi\right)\right)\right)i_q-\frac{2}{3}\Delta_{M_0}\sin\left(2\theta-\frac{2}{3}\pi\right)i_d\end{aligned} \quad (2.26)$$

Separate the equation (2.26) into 2 components representing the magnetic part that is not affected and the one affected by the end effect as follows

$$\begin{bmatrix}\psi_{d0}\\ \psi_{q0}\end{bmatrix}=\begin{bmatrix}L_{d1} & L_{dq1}\\ L_{qd1} & L_{q1}\end{bmatrix}\begin{bmatrix}i_d\\ i_q\end{bmatrix}=\begin{bmatrix}L_0+\frac{1}{2}L_2-M_0+M_2 & 0\\ 0 & L_0-\frac{1}{2}L_2-M_0-M_2\end{bmatrix}\begin{bmatrix}i_d\\ i_q\end{bmatrix} \quad (2.27)$$

$$\begin{bmatrix}\Delta\psi_d\\ \Delta\psi_q\end{bmatrix}=\begin{bmatrix}L_{d2} & L_{dq2}\\ L_{qd2} & L_{q2}\end{bmatrix}\begin{bmatrix}i_d\\ i_q\end{bmatrix}=-\frac{2}{3}\Delta_{M_0}\begin{bmatrix}1+\cos\left(2\theta-\frac{2}{3}\pi\right) & -\sin\left(2\theta-\frac{2}{3}\pi\right)\\ -\sin\left(2\theta-\frac{2}{3}\pi\right) & 1-\cos\left(2\theta-\frac{2}{3}\pi\right)\end{bmatrix}\begin{bmatrix}i_d\\ i_q\end{bmatrix} \quad (2.28)$$

Finding that (2.28) is the magnetic flux model influenced by the end effect in the 3-phase LPMSM in the *dq* coordinates. In which the component Δ_{M0} is estimated from experiment results based on equations (2.23) and (2.24)

2.3 Mathematic description of Polysolenoid LPMSM

2.3.1 Model of equivalent magnetic circuit

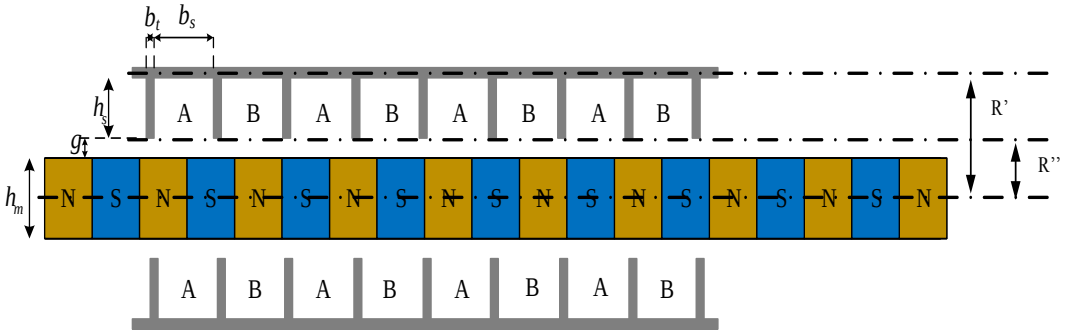

Hình 2.11 Side view of the Polysolenoid LPMSM

In general, the reluctance is calculated by: $R_m=\frac{l_c H}{A_c B}$ (2.30)

The leakage reluctance is calculated as follows: $R_{m\sigma} = \dfrac{2b_s}{\mu_0 h_s l_s}$ (2.32)

where h_s is the height of the winding slot. With the structure of the polysolenoid linear motor: $l_s = 2\pi \dfrac{R' + R''}{2}$ (2.33)

R', R": is the outer radius and the inner radius of the part containing windings in the slots grooves from the center according to the section of the motor.

The secondary part (slider) of the motor is made from the magnetic material NdFeB N38UH. The parameters based on the manufacturer's documents combined with [62] we obtained the B-H characteristic according to Fig. 2.12.

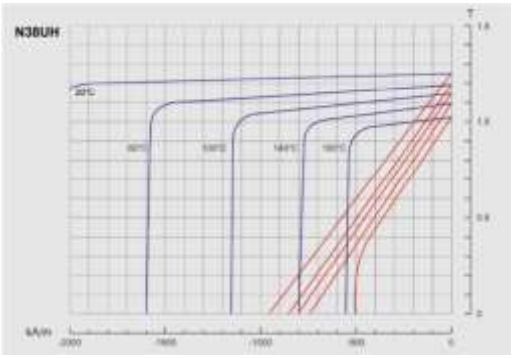

Fig. 2.12 The B-H curve of NdFeB N38UH material [61]

Based on the B-H characteristic we have:

The reluctance of the winding slot: $R_{mt} = \dfrac{h_s}{b_t.2\pi.R'} \dfrac{H}{B_t}$ (2.34)

The reluctance of the winding: $R_{my} = \dfrac{h_s}{b_s.2\pi.R'} \dfrac{H}{B_y}$ (2.35)

Permanent magnet flux: $\begin{cases} \Phi_{pma} = \hat{\Phi}_{pm} \cos\left(\dfrac{\pi}{\tau_p} x\right) \\ \Phi_{pmb} = \hat{\Phi}_{pm} \cos\left(\dfrac{\pi}{\tau_p} x - \dfrac{\pi}{2}\right) \end{cases}$ (2.36)

Electromagnetic force: $\begin{cases} F_{mpma} = R_{mg} \Phi_{pma} \\ F_{mpmb} = R_{mg} \Phi_{pmb} \end{cases}$ (2.37)

The stator voltage is written as follows (assuming the motor has 4 polar pairs):

$$\begin{cases} u_a = Ri_a + N_t \dfrac{d}{dt}(\Phi_{a1} + \Phi_{a2} + \Phi_{a3} + \Phi_{a4}) \\ u_b = Ri_b + N_t \dfrac{d}{dt}(\Phi_{b1} + \Phi_{b2} + \Phi_{b3} + \Phi_{b4}) \end{cases} \quad (2.38)$$

From (2.31), (2.32), (2.34), (2.37), (2.38) a equivalent magnetic circuit diagram is built as shown in Fig. 2.13

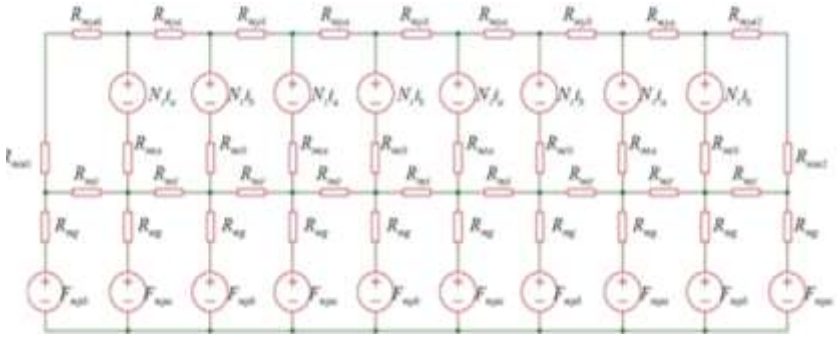

Fig. 2.13 Equivalent magnetic circuit of a 4 pole pairs linear motor considering the end effect

2.3.2 Proposed differential equation system

Based on calculations of equivalent magnetic circuit in Fig. 2.13.

$$\begin{cases} u_d = R_s i_d + L_{sd}\dfrac{di_d}{dt} - \omega_e L_q i_q + \Delta L_d(\theta)\dfrac{di_d}{dt} + L_{dq}(\theta)\dfrac{di_q}{dt} - \omega_e\left(\Delta L_q(\theta) i_q + L_{dq}(\theta) i_d - \dfrac{\partial \Delta L_d(\theta)}{\partial\theta} i_d - \dfrac{\partial L_{dq}(\theta)}{\partial\theta} i_q\right) \\ u_q = R_s i_q + L_{sq}\dfrac{di_q}{dt} - \omega_e L_d i_d - \omega_e \psi_p + \Delta L_q(\theta)\dfrac{di_q}{dt} + L_{dq}(\theta)\dfrac{di_d}{dt} - \omega_e\left(\Delta L_d(\theta) i_d + L_{dq}(\theta) i_q - \dfrac{\partial \Delta L_q(\theta)}{\partial\theta} i_q - \dfrac{\partial L_{dq}(\theta)}{\partial\theta} i_d\right) \end{cases} \quad (2.49)$$

Transform (2.49) into the form of first order differential equation with variables are current vector and voltage vector in *d-q* coordinates:

$$\mathbf{u}_{dq} = \mathbf{R}\mathbf{i}_{dq} + \mathbf{L}(\theta)\frac{d}{dt}\mathbf{i}_{dq} + \mathbf{L}_1(\theta)\omega_e \mathbf{i}_{dq} - \mathbf{G}\psi_p\omega_e \quad (2.50)$$

where:

$$\mathbf{u}_{dq} = \begin{bmatrix} u_d \\ u_q \end{bmatrix}; \mathbf{i}_{dq} = \begin{bmatrix} i_d \\ i_q \end{bmatrix}; \mathbf{R} = \begin{bmatrix} R_s & 0 \\ 0 & R_s \end{bmatrix}; \mathbf{L}(\theta) = \begin{bmatrix} L_d(\theta) & L_{dq}(\theta) \\ L_{dq}(\theta) & L_q(\theta) \end{bmatrix}; \mathbf{G} = \begin{bmatrix} 0 \\ 1 \end{bmatrix}$$

$$\mathbf{L}_1(\theta) = \begin{bmatrix} \dfrac{\partial \Delta L_d(\theta)}{\partial\theta} - L_{dq}(\theta) & \dfrac{\partial L_{dq}(\theta)}{\partial\theta} - L_q(\theta) \\ \dfrac{\partial L_{dq}(\theta)}{\partial\theta} + L_d(\theta) & \dfrac{\partial \Delta L_q(\theta)}{\partial\theta} + L_{dq}(\theta) \end{bmatrix}$$

Convert (2.50) to the form:

$$\frac{d\mathbf{i}_{dq}}{dt} = -\mathbf{L}^{-1}\mathbf{R}\mathbf{i}_{dq} - \mathbf{L}^{-1}\mathbf{L}_1\mathbf{i}_{dq}\omega_e + \mathbf{L}^{-1}\mathbf{G}\psi_p\omega_e + \mathbf{L}^{-1}\mathbf{u}_{dq} \quad (2.51)$$

$$\begin{cases} \dfrac{d\mathbf{i}_{dq}}{dt} = -\mathbf{L}^{-1}\mathbf{R}\mathbf{i}_{dq} - \mathbf{L}^{-1}\mathbf{L}_1\mathbf{i}_{dq}\omega_e + \mathbf{L}^{-1}\mathbf{G}\psi_p\omega_e + \mathbf{L}^{-1}\mathbf{u}_{dq} \\ \dfrac{d\omega_e}{dt} = \dfrac{1}{m}\left(\psi_p i_q + \left(L_d(\theta) - L_q(\theta)\right) i_d i_q + L_{dq}(\theta)\left(i_q^2 - i_d^2\right)\right) - \left(\dfrac{\tau_p}{2\pi m}\right) F_c \end{cases} \quad (2.56)$$

From the differential equation, the structure diagram describing the components in the *dq* coordinate system with the desire to clarify the physical nature as well as the MIMO nature of the object.

Set:

$$T_q = \frac{L_q}{R_s}, T_d = \frac{L_d}{R_s}; \sigma = 1 - L_{dq}^2 / L_d L_q, \mathbf{L}(\theta)^{-1} = \frac{1}{L_d L_q - L_{dq}^2}\begin{bmatrix} L_q & -L_{dq} \\ -L_{dq} & L_d \end{bmatrix} = \begin{bmatrix} \frac{1}{\sigma L_d} & \frac{-L_{dq}}{L_d L_q \sigma} \\ \frac{-L_{dq}}{L_d L_q \sigma} & \frac{1}{\sigma L_q} \end{bmatrix},$$

$$\mathbf{L}^{-1}(\theta)\mathbf{L}_1(\theta) = \begin{bmatrix} \frac{1}{\sigma L_d} & \frac{-L_{dq}}{L_d L_q \sigma} \\ \frac{-L_{dq}}{L_d L_q \sigma} & \frac{1}{\sigma L_q} \end{bmatrix}\begin{bmatrix} c_1 & c_2 \\ c_3 & c_4 \end{bmatrix} = \begin{bmatrix} \frac{c_1}{\sigma L_d} - \frac{L_{dq} c_3}{L_d L_q \sigma} & \frac{c_2}{\sigma L_d} - \frac{L_{dq} c_4}{L_d L_q \sigma} \\ \frac{c_3}{\sigma L_q} - \frac{L_{dq} c_1}{L_d L_q \sigma} & \frac{c_4}{\sigma L_q} - \frac{L_{dq} c_2}{L_d L_q \sigma} \end{bmatrix}$$

The equation (2.56) leads to:

$$\begin{cases} \frac{di_{sd}}{dt} = -\frac{1}{\sigma T_d} i_d + \frac{L_{dq}}{\sigma L_q T_d} i_q + \omega_e \left(\frac{c_3 L_{dq}}{\sigma L_d L_q} - \frac{c_1}{\sigma L_d} \right) i_d + \omega_e \left(\frac{c_4 L_{dq}}{\sigma L_d L_q} - \frac{c_2}{\sigma L_d} \right) i_q + \frac{1}{\sigma L_d} u_d - \frac{L_{dq}}{\sigma L_d L_q} u_q \\ \frac{di_{sq}}{dt} = -\frac{1}{\sigma T_q} i_q + \frac{L_{dq}}{\sigma L_d T_q} i_d + \omega_e \left(\frac{c_1 L_{dq}}{\sigma L_d L_q} - \frac{c_3}{\sigma L_q} \right) i_d + \omega_e \left(\frac{c_2 L_{dq}}{\sigma L_d L_q} - \frac{c_4}{\sigma L_q} \right) i_q - \frac{1}{\sigma L_q} \omega_e \psi_p + \frac{1}{\sigma L_q} u_q - \frac{L_{dq}}{\sigma L_d L_q} u_d \end{cases} \quad (2.57)$$

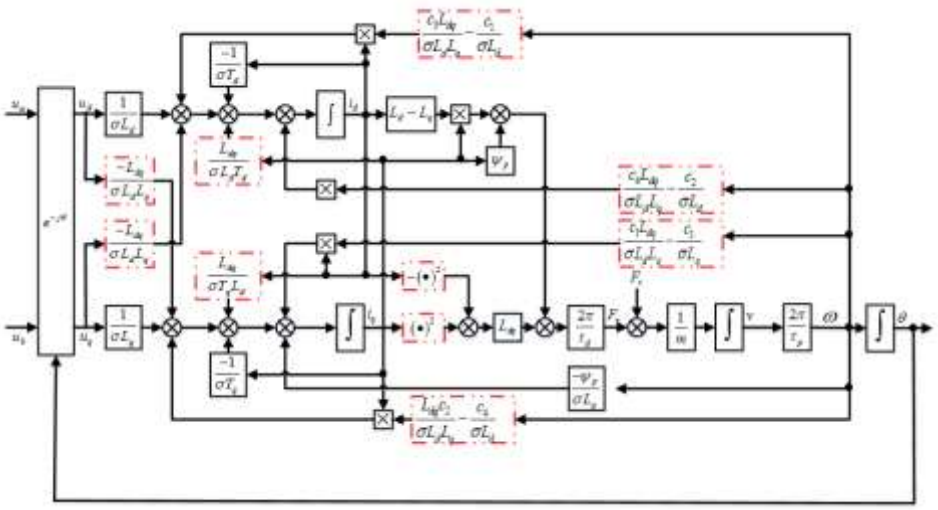

Fig. 2.15 Structure diagram of the polysolenoid LPMSM in the *dq* coordinate system

Conclusion of chapter 2:

The results of Chapter 2 solved the problem of building a unified model of a polysolenoid linear permanent magnet synchronous motor considering end effect. The obtained model is the premise in designing control for the drive system using polysolenoid linear permanent magnet synchronous motor. This is the next content of the thesis.

CHAPTER 3 : CONTROL OF POLYSOLENOID LINEAR MOTOR

3.1 Overview of control structure

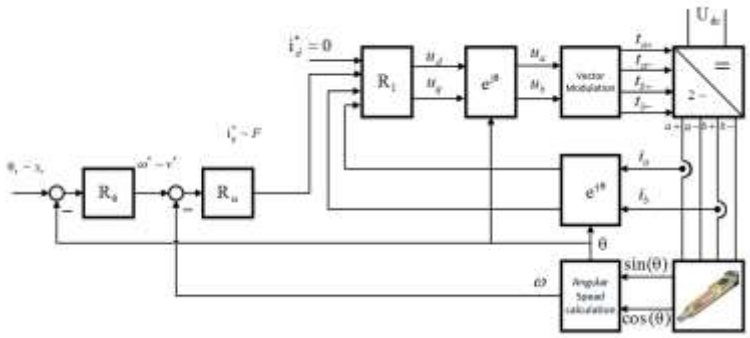

Figure 3.1 Structure diagram of FOC applied to 2-phase linear motor which is supplied by 2 independent power supply

3.2 Control methods (current control)

3.2.1 New deadbeat control method

In this section, the author presents how to design the stator current controller in a completely new direction to ensure quality criteria such as: decoupling, stator current reachs reference during the finite time period (FAT) has been successfully designed according to [1].

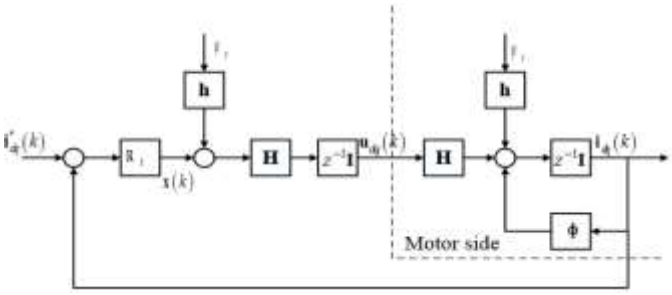

Fig. 3.2 Bock diagram of the deadbeat stator current control loop in the rotor flux oriented coordinates

$$\mathbf{R_I}\left(z^{-1}\right)=\begin{bmatrix} \dfrac{\left(z-\Phi_{11}\right)P_1\left(z^{-1}\right)}{1-z^{-1}P_1\left(z^{-1}\right)} & \dfrac{-\Phi_{12}P_2\left(z^{-1}\right)}{1-z^{-1}P_2\left(z^{-1}\right)} \\ \dfrac{-\Phi_{21}P_1\left(z^{-1}\right)}{1-z^{-1}P_1\left(z^{-1}\right)} & \dfrac{\left(z-\Phi_{22}\right)P_2\left(z^{-1}\right)}{1-z^{-1}P_2\left(z^{-1}\right)} \end{bmatrix} \tag{3.17}$$

3.2.2 Predictive control MPC

Different from traditional optimal control where the optimal solution is established based on the solution of the given optimal problems. Therefore, it is difficult to react to non-predetermined changes of the system such as noise, model deviation ... The optimal control signal according to MPC is a sequence of control signals, each of which represents for control signals at the k time. The optimal problem is repeated at each cycle with the latest information about the system. Fig. 3.1 below shows the basic configuration of the model predictive control system.

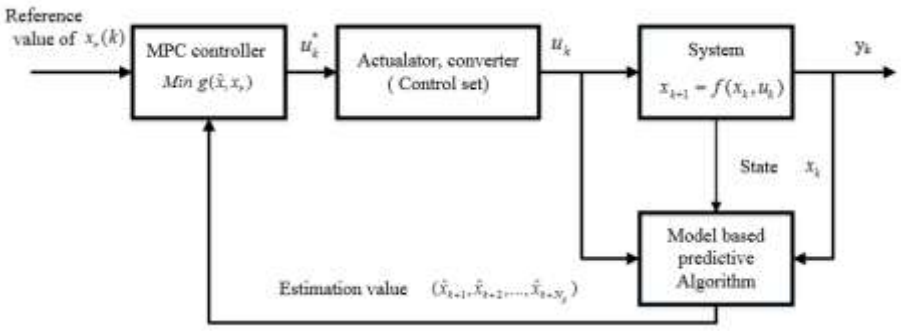

Fig. 3.3 Structure diagram of MPC system

In addition, based on the properties of the actuator or more specifically in this thesis are the converter and their control methods, in this section we propose two different predictive control schemes based on continuous and discrete (finite) nature of elements in the control set.

- If the voltage applied to the two motor windings is considered as continuous, the modulation limit leads to the voltage being in the bounded, continuous set. This results in a predictive control method with Continuous control set MPC (CCS MPC).

- Considering the instantaneous voltage on the motor, consider the converter to be ideal leading to a finite control voltage set depending on the converter configuration. This takes on the predictive control method with finite control set (Finite control set MPC - FCS MPC).

MPC with continuous control set

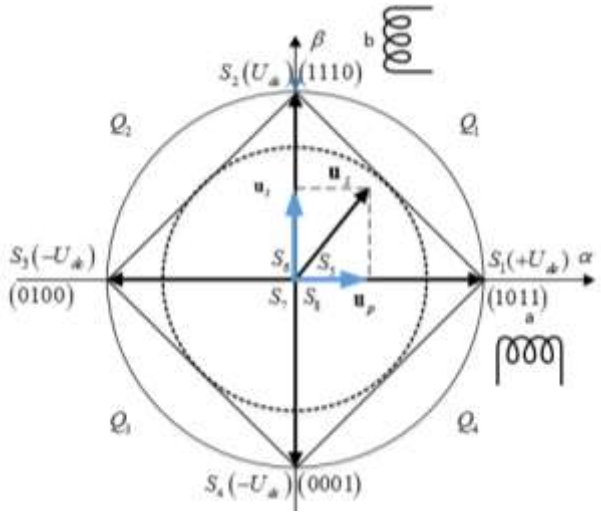

Fig. 3.5 Modulation plane in α,β coordinates according to CCS-MPC method

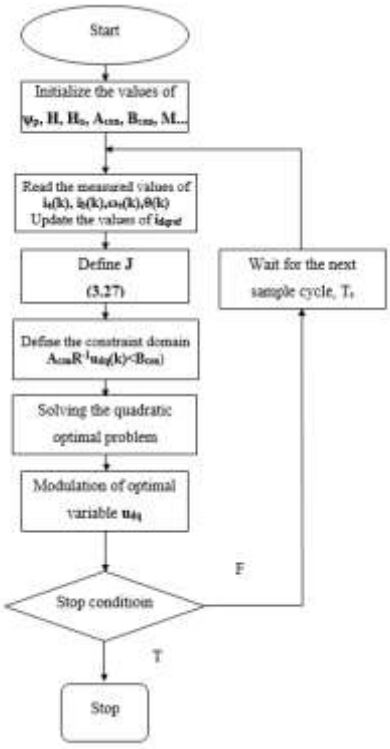

Fig. 3.6 Flowchart of CCS-MPC controller

To form the modulation domain, the formula system is used:

$$\begin{aligned}
&\mathbf{u}_s = \mathbf{u}_p + \mathbf{u}_t \\
&\mathbf{u}_s \in Q_1 : \left|\mathbf{u}_p\right| = \frac{T_p}{T_{pulse}} U_{dc};\ \left|\mathbf{u}_t\right| = \frac{T_t}{T_{pulse}} U_{dc}; \mathbf{u}_s \in Q_2 : \left|\mathbf{u}_p\right| = -\frac{T_p}{T_{pulse}} U_{dc};\ \left|\mathbf{u}_t\right| = \frac{T_t}{T_{pulse}} U_{dc} \\
&\mathbf{u}_s \in Q_3 : \left|\mathbf{u}_p\right| = -\frac{T_p}{T_{pulse}} U_{dc};\ \left|\mathbf{u}_t\right| = -\frac{T_t}{T_{pulse}} U_{dc}; \mathbf{u}_s \in Q_4 : \left|\mathbf{u}_p\right| = \frac{T_p}{T_{pulse}} U_{dc};\ \left|\mathbf{u}_t\right| = -\frac{T_t}{T_{pulse}} U_{dc} \\
&T_p + T_t + T_{off} = T_{pulse}
\end{aligned} \tag{3.22}$$

MPC with finite control set

For objects with discrete nature such as power converters, FCS MPC method proved very effective. It provides a completely different approach to power converters. This method is based on the finite number of permissible valve combinations of the power converter.

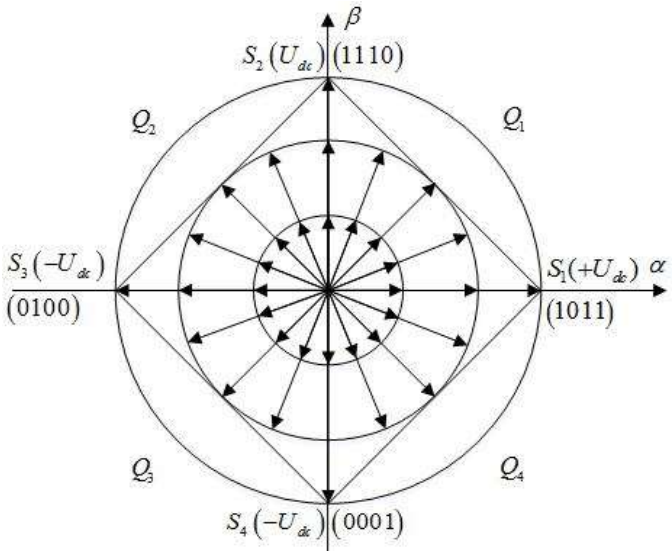

Fig. 3.7 Modulation plane in α,β coordinates according to FCS-MPC method

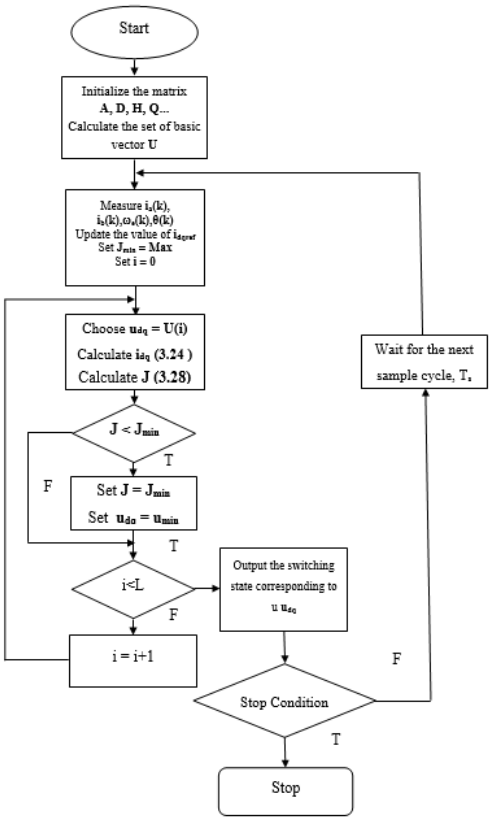

Fig. 3.8 Flowchart of FCS-MPC controller

3.3 Outer loop controller Min-Max MPC

3.4 Backstepping adaptive design

From the motor model (2.49), combined with the approximation rule (3.42), the following equation system is obtained:

$$\begin{cases} u_d = R_s i_d - \omega_e \left(\left(A_{1dq} \sin 2\theta + B_{1dq} \cos 2\theta \right) i_d + \left(L_q + A_{1q} \sin 2\theta + B_{1q} \cos 2\theta \right) i_q \right) \\ \quad + 2\omega_e \left(A_{1d} \cos 2\theta - B_{1d} \sin 2\theta \right) i_d + 2\omega_e \left(A_{1dq} \cos 2\theta - B_{1dq} \sin 2\theta \right) i_q \\ \quad + \left(L_d + A_{1d} \sin 2\theta + B_{1d} \cos 2\theta \right) \dfrac{di_d}{dt} + \left(\left(A_{1dq} \sin(2\theta) + B_{1dq} \cos 2\theta \right) \right) \dfrac{di_q}{dt} \\ u_q = R_s i_q + \omega_e \left(\left(L_d + A_{1d} \sin 2\theta + B_{1d} \cos 2\theta \right) i_d + \left(A_{1dq} \sin 2\theta + B_{1dq} \cos 2\theta \right) i_q + \psi_p \right) \\ \quad + 2\omega_e \left(A_{1dq} \cos 2\theta - B_{1dq} \sin 2\theta \right) i_d + 2\omega_e \left(A_{1q} \cos 2\theta - B_{1q} \sin 2\theta \right) i_q \\ \quad + \left(A_{1dq} \sin 2\theta + B_{1dq} \cos 2\theta \right) \dfrac{di_d}{dt} + \left(L_q + A_{1q} \sin 2\theta + B_{1q} \cos 2\theta \right) \dfrac{di_q}{dt} \end{cases}$$

Rewrite the above system of equations as matrices:

$$\mathbf{M} \frac{d\mathbf{i}_{dq}}{dt} = \mathbf{u}_{dq} + \mathbf{G} + \mathbf{H} \tag{3.43}$$

where:

$$\mathbf{i}_{dq} = \begin{bmatrix} i_d & i_q \end{bmatrix}^T, \mathbf{u}_{dq} = \begin{bmatrix} u_d & u_q \end{bmatrix}^T; \mathbf{M} = \begin{bmatrix} L_d + A_{1d} \sin(2\theta) + B_{1d} \cos(2\theta) & \left(A_{1dq} \sin(2\theta) + B_{1dq} \cos(2\theta) \right) \\ \left(A_{1dq} \sin(2\theta) + B_{1dq} \cos(2\theta) \right) & \left(L_q + A_{1q} \sin(2\theta) + B_{1q} \cos(2\theta) \right) \end{bmatrix}$$

$$\mathbf{G} = \begin{bmatrix} -R_s i_d \\ -R_s i_q - \omega_e \psi_p \end{bmatrix}; \mathbf{H} = \begin{bmatrix} \begin{pmatrix} \omega_e \left[\left(A_{1dq} \sin(2\theta) + B_{1dq} \cos(2\theta) \right) i_d + \right. \\ \left. \left(A_{1q} \sin(2\theta) + B_{1q} \cos(2\theta) \right) i_q \right] + \omega_e L_q i_q - \\ 2\omega_e \left(A_{1d} \cos(2\theta) - B_{1d} \sin(2\theta) \right) i_d - \\ 2\omega_e \left(A_{1dq} \cos(2\theta) - B_{1dq} \sin(2\theta) \right) i_q \end{pmatrix} \\ \begin{pmatrix} -\omega_e \left[\left(A_{1d} \sin(2\theta) + B_{1d} \cos(2\theta) \right) i_d + \right. \\ \left. \left(A_{1dq} \sin(2\theta) + B_{1dq} \cos(2\theta) \right) i_q \right] - \omega_e L_d i_d - \\ 2\omega_e \left(A_{1dq} \cos(2\theta) - B_{1dq} \sin(2\theta) \right) i_d + \\ 2\omega_e \left(A_{1q} \cos(2\theta) - B_{1q} \sin(2\theta) \right) i_q \end{pmatrix} \end{bmatrix}$$

In this section, adaptive controller is designed with undefined inductances in (3.42). Since $\mathbf{M} = \mathbf{M}(\theta)$ is positive-definite matrix, $\mathbf{G} = \mathbf{G}\left(\mathbf{i}_{dq}, \omega_e\right), \mathbf{H} = \mathbf{H}\left(\mathbf{i}_{dq}, \omega_e, \theta\right)$, the equation system (3.44),(3.45),(3.46) have the form of below triangle as the following:

$$\begin{aligned} &\frac{d\theta}{dt} = \omega_e \\ &\frac{d\omega_e}{dt} = \mathbf{E}\mathbf{i}_{dq} - \frac{2\pi}{m\tau_p} F_c \\ &\frac{d\mathbf{i}_{dq}}{dt} = \mathbf{h}\left(\theta, \omega_e, \mathbf{i}_{dq}\right) + \mathbf{M}^{-1}(\theta)\mathbf{u}_{dq} \end{aligned} \tag{3.47}$$

where $\mathbf{h}\left(\theta,\omega_e,\mathbf{i}_{dq}\right)=\mathbf{M}^{-1}\left(\theta\right)\left(\mathbf{G}\left(\mathbf{i}_{dq},\omega_e\right)+\mathbf{H}\left(\mathbf{i}_{dq},\omega_e,\theta\right)\right)$. At this point, we have enough basis to conduct backstepping control design for the above equation system.

Select the virtual speed control signal as follows:

$$\omega_c=\omega_r-k_\theta e_\theta \tag{3.51}$$

With the virtual current control signal:

$$i_{qc}=-k_\omega\tilde{\omega}+a^{-1}\dot{\omega}_c-e_\theta \tag{3.56}$$

Choose voltage control signal:

$$\mathbf{u}_{dq}=-\mathbf{\Gamma}\tilde{\mathbf{i}}_{dq}-\mathbf{G}-\mathbf{Y}\hat{\boldsymbol{\xi}}-\begin{bmatrix}0 & \tilde{\omega}\end{bmatrix}^T \tag{3.62}$$

And adaptive control rule:

$$\dot{\hat{\boldsymbol{\xi}}}=\mathbf{\Pi}\left(-\beta\hat{\boldsymbol{\xi}}+\mathbf{Y}^T\tilde{\mathbf{i}}_{dq}\right) \tag{3.63}$$

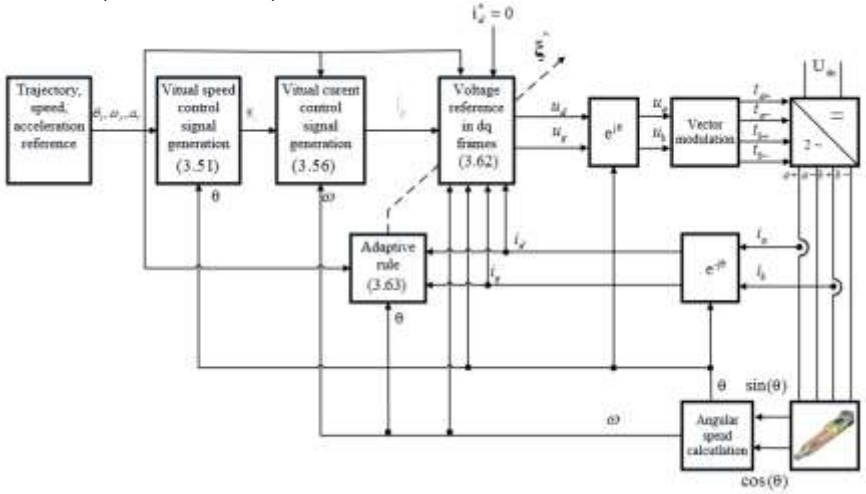

Fig. 3.9 Structure diagram of Polysolenoid linear motor control system based on backstepping adaptive control

Conclusion of chapter 3

The whole position control structure for polysolenoid linear motor has been presented in chapter 3 including 2 groups of methods of MPC and backstepping adaptive control. In the MPC method group, the author has designed the control structure of inner and outer control loops. The current control loop is proposed with 3 main controllers, deadbeat, CCS-MPC, and FCS-MPC. With the speed and position control loop uses the Min-Max MPC controller. In order to solve the problem of end effect, backstepping adaptive control method to approximate the effect of end effect through the change in stator inductance. In the next section, simulation and experimental results are used to compare the quality of the proposed methods.

CHAPTER 4 : SIMULATION AND EXPERIMENT RESULTS

The simulation is implemented in the following scenario:

- Reference: consider the sinusoidal trajectory and trajectory with rectangular waveform of speed.
- Load: consider the operation of the motor with and without load.
- Motor model: with end effect and without end effect.

4.1 Simulation results

4.1.1 System simulation with the outer loop Min-Max MPC, current loop FCS-MPC

Parameters of FCS-MPC current controller: current sample time $T_i = 50(\mu s)$; $\mathbf{Q} = \mathbf{diag}([10\ 1])$; Parameters of MinMax-MPC speed controller: speed sample time $T_w = 2000(\mu s)$; $\mathbf{Q} = \mathbf{diag}([10\ 0.01])$; predictive range $N_w = 6$; State feefback matrix $K = [800\ 1]$; friction coefficient $c_f = 0.1;\ N_p = 2$

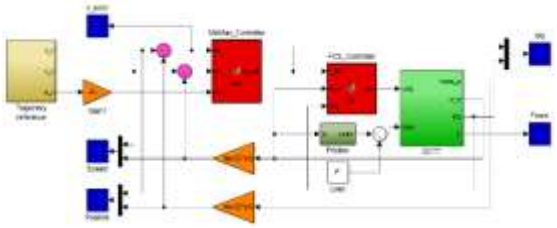

Fig. 4.1 Simulation diagram of Min Max-FCS MPC controller without considering end effect

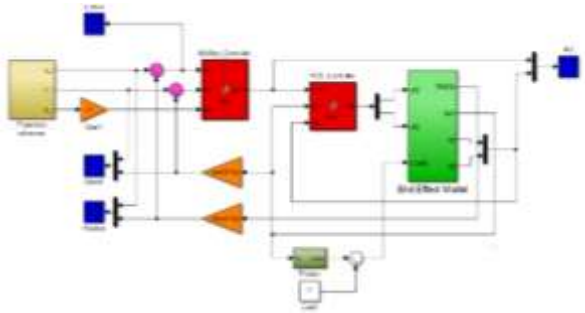

Fig. 4.2 Simulation diagram of Min Max-FCS MPC controller with considering end effect

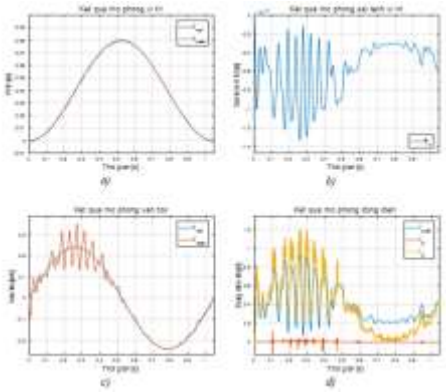

Fig. 4.6 Simulation results of Min Max-FCS MPC controller with sinusoidal reference trajectory: with load, with end effect

4.1.2 System simulation with the outer loop Min-Max MPC, current loop CCS-MPC

Parameters of CCS-MPC current controller: current sample time $T_i = 100(\mu s)$; $\mathbf{Q} = \mathbf{diag}([10\ 1])$. Parameters of MinMax-MPC speed, posistion controller: speed sample time $T_w = 2000(\mu s)$; $\mathbf{Q} = \mathbf{diag}([10\ 0.01])$; predictive range $N_w = 6$; State feefback matrix $K = [800\ 1]$; friction coefficient $c_f = 0.1; N_p = 1.$

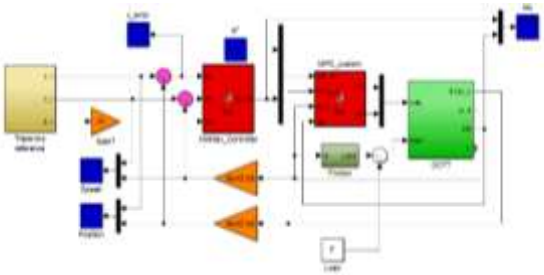

Fig. 4.11 Simulation results of Min Max-CCS MPC controller with sinusoidal reference trajectory: with load, without end effect

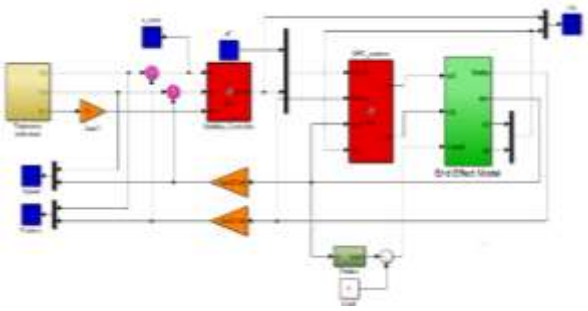

Fig. 4.12 Simulation diagram of Min Max-CCS MPC controller with considering end effect

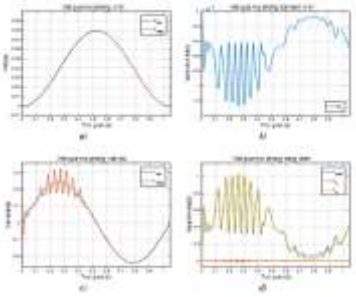

Fig. 4.16 Simulation results of Min Max-CCS MPC controller with sinusoidal reference trajectory: with load, with end effect

4.1.3 System simulation with the outer loop Min-Max MPC, dead-beat current control loop

Parameters of CCS-MPC Dead-beat current controller: current sample time; $T_i = 50(\mu s)$, the order of $L(z^{-1})$ is 2, $l_1 = l_2 = 0.5$. Parameters of MinMax-MPC speed, posistion controller: speed sample time $T_w = 2000(\mu s)$; $\mathbf{Q} = \mathbf{diag}([10\ 0.01])$; predictive range $N_w = 6$; State feefback matrix $K = [800\ 1]$; friction coefficient $c_f = 0.1$;

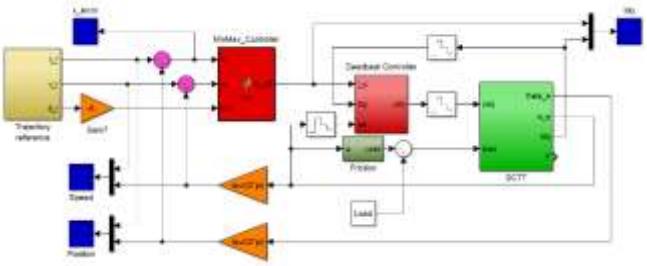

Fig. 4.21 Simulation diagram of Min Max MPC – Deadbeat controller without considering end effect

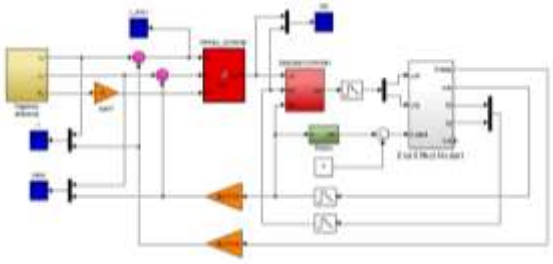

Fig. 4.22 Simulation diagram of Min Max MPC –Deadbeat controller with considering end effect

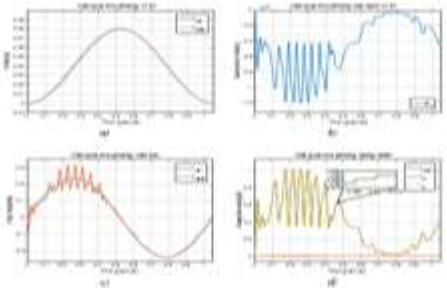

Fig. 4.26 Simulation results of Min Max MPC –Deadbeat controller with sinusoidal reference trajectory: with load, with end effect

4.1.4 System simulation with adaptive backstepping controller

Sample time $T_s = 0.15(ms)$, Adaptive controller parameters: $\beta = 0.01$, $k_\theta = 50, k_\omega = 0.01$; $\mathbf{\Pi} = \mathbf{diag}([0.1,...,0.1])$; $\mathbf{\Gamma} = \mathbf{diag}([500 \quad 500])$

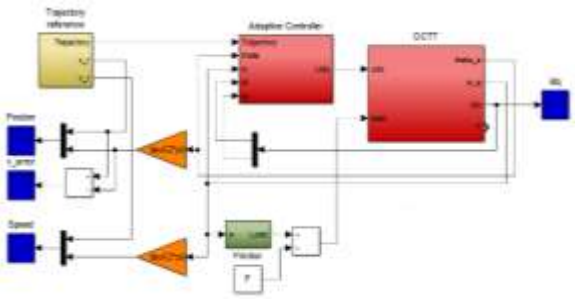

Fig. 4.31 Simulation diagram of adaptive backstepping controller without considering end effect

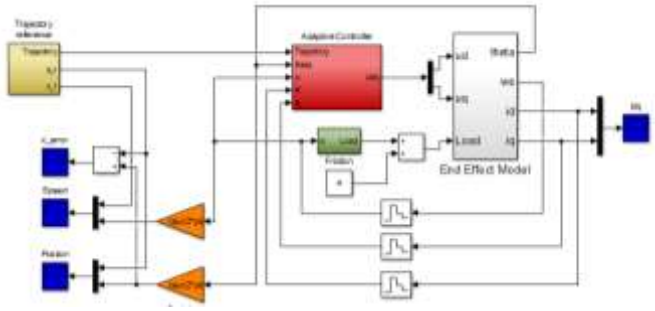

Fig. 4.32 Simulation diagram of adaptive backstepping controller with considering end effect

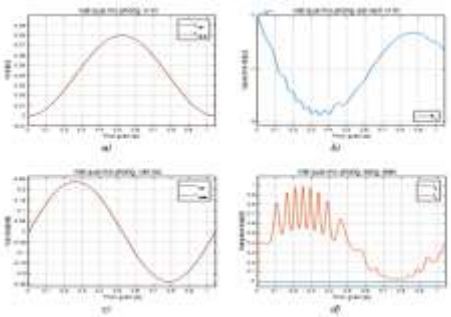

Fig. 4.36 Simulation results of adaptive backstepping controller with sinusoidal reference trajectory: with load, with end effect

4.2 Experimental results

The experimental part of the thesis is presented in detail in the appendix. The experiments use the same trajectory as in the simulation. There are two types of orbits that are used: sinusoidal trajectory and the trajectory with step speed.

Fig. 4.41 Experiment System

To verify the performance of the controller, the load used in this thesis is a potential load, the load is constant throughout the working process.

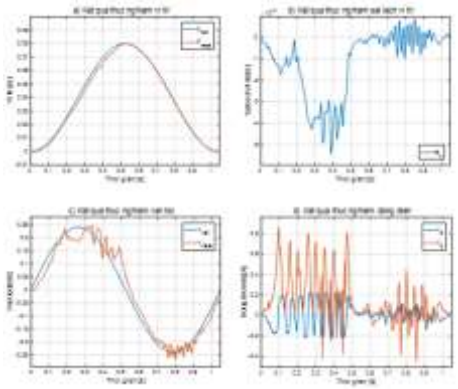

Fig. 4.44 Experimental results of Min Max-FCS MPC controller with sinusoidal trajectory reference: with load

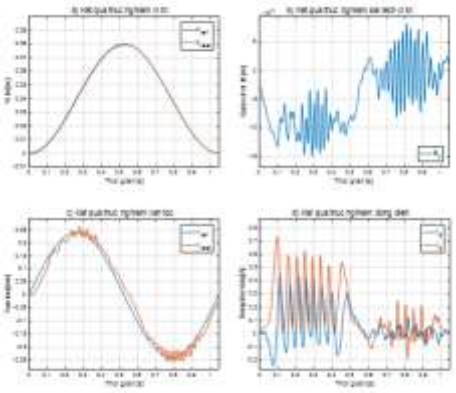

Fig. 4.48 Experimental results of Min Max-CCS MPC controller with sinusoidal trajectory reference: with load

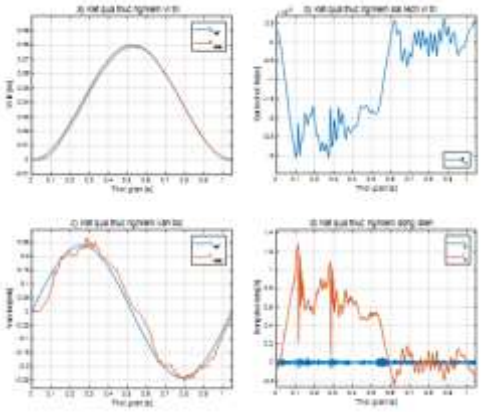

Fig. 4.52 Experimental results of Min Max-Deadbeat controller with sinusoidal trajectory reference: with load

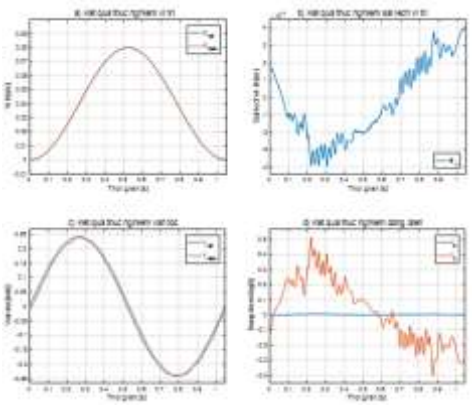

Fig. 4.56 Experimental results of Backstepping controller with sinusoidal trajectory reference: with load

4.3 Remarks on simulation and experimental results

The methods presented in the thesis are divided into two groups of methods:

The first group (without considering the end effect in control design) includes: Min max FCS - MPC, Min max CCS - MPC, Min max Deadbeat. In these methods, the parameters of the controller must be designed based on the exact parameters of the motor so the inductance component is constant.

The second group (the end effect is not taken into account in control design): Backstepping adaptive design method. Adaptative law is used to counteract the variable value of inductance during motor operation.

Table 4.1 Comparison of control quality of controllers (+: good)

Outer loop controller	Current controller	Accuracy	Current decoupling effect	μP computing capability	Condition of design usage

Min max MPC	FCS-MPC	+	+	++++	Without end effect
	CCS-MPC	++	++	+++	
	Dead beat	+++	+++	++	
Adaptive Back Stepping		++++	++++	+	With end effect

Experimental results show the advantages of backstepping adaptive design methods that provide position accuracy as well as effective current decoupling. However, the disadvantage of backstepping method is that it requires high power microprocessor.

The results:

Table 4.1. Simulation and experiment results

Control method	Trajectory	Sin				Linear			
	Load	x	x	o	o	x	o	x	o
	Effect	x	o	x	o	x	o	o	x
FCS	Simulation	0.26	0.33	0.51	0.56	0.18	0.21	0.57	0.52
	Experiment	-	0.63	-	1.2	-	0.29	1.3	-
CCS	Simulation	0.25	0.27	0.45	0.48	0.14	0.15	0.49	0.45
	Experiment	-	0.41	-	0.53	-	0.25	0.99	-
Deadbeat	Simulation	0.25	0.27	0.42	0.45	0.14	0.15	0.46	0.42
	Experiment	-	0.30	-	0.32	-	0.24	0.62	-
Backstepping	Simulation	0.03	0.03	0.10	0.10	0.05	0.05	0.11	0.11
	Experiment	-	0.17	-	0.19	-	0.067	0.38	-

CONCLUSIONS AND RECOMMENDATIONS

A. CONCLUSIONS

Linear Permanent Magnet Synchronous Motor (LPMSM) is widely used in industry due to the properties such as providing direct linear motion, high power density, durability and precision. Different from rotary motor, end effect is a characteristic phenomenon only found in linear motor due to its unique geometric structure with opened magnetic circuit structure. Most control methods that have been applied to linear motors ignore the end effect in the control structure. This thesis focuses on the study of polysolenoid permanent magnet linear motors considering the end effect in modeling and control design. Polysolenoid motors are a special type of permanent magnet linear motors with a tubular structure especially suitable for parallel robot objects such as hexapods. Implementing the research tasks set out in the thesis topic is structured in turn according to the sequence: overview study on the principles, operation principles, applications in practice of linear motor, control methods that have been applied to this technology object. All of these things with the aim of creating an overall picture of the research situation up to now from which to orient the next path and to serve the next part of the thesis that is Polysolenoid motors simulation. Polysolenoid motor is a kind of LPMSM, so a model of LPMSM is built before considering the Polysolenoid motor model in particular. The Polysolenoid motor model is established based on the general knowledge, after that the end effect component is added to the model. The next task is control design with and without considering end effect. The simulation and experimental results are used to verify the correctness of the proposed theory.

New Contributions of the thesis

- The thesis has built a mathematical model of Polysolenoid motor considering the end effect for control design. The model with end effect of the Polysolenoid motor has been built on the basis of the magnetic equivalent circuit (MEC), based on the conversion of the magnetic circuit to the electric circuit. The equivalent resistance values are calculated and then an electric equivalent circuit model is established, showing the flux changes through the inductance value of the motor depending on the position of the secondary part. From the magnetic equivalent circuit model, the differential equation model of the Polysolenoid LPMSM is set up in the *dq* coordinate system. The results are the system of differential equations and structure diagram of the Polysolenoid LPMSM considering end effect used in the control.
- The next contribution of the thesis is the design of the backstepping adaptive controller (single loop control structure) to handle the end effect of the Polysolenoid motor.

- Final contribution of the thesis: the author has designed the two-loop control structure in which the inner loop is the force (current) control using control methods of Dead-beat, CCS-MPC, FCS -MPC; outer control loop is the speed and position control using the Min-max MPC controller. In control design, these methods do not take into account the end effect in the mathematical model but they are the most dynamically dominant and capable of reducing the amount of calculation for the microcontroller. These methods will be used to compare the control quality with the Backstepping control method in the experiment. This is appropriate because when the experiment is conducted, the object here is the real motor (with the physical nature that the end effect always exists) so the controllers must respond to the real object performances, not the ideal object in the simulation model.

B. RECOMMENDATIONS

The thesis has solved the research objectives and tasks with some new contributions. However, on the basis of the research results, there are some problems that need to further study in the future.

- Continue to study nonlinear control algorithms for Polysolenoid LPMSM on the basis of the proposed mathematical model and experiment.
- Continue to study to find measurement method in order to accurately determine the changing value of the inductance of the motor during operation. The success in identifying inductances will provide a table of data about the value of inductance in motion (LUT). The access of the inductance values to directly add to the mathematical model will solve the specific characteristics of the end effect of a linear motor. Then the control design methods for synchronous ac motors can be completely applied to LPMSM
- Deployment of research results on Polysolenoid motors for parallel robot systems, namely Hexapod system, manipulator control.